

PHASE INTERMODULATION DISTORTION -  
INSTRUMENTATION AND MEASUREMENT RESULTS

Robert R. Cordell  
Bell Laboratories  
Holmdel, N.J. 07733

Phase intermodulation (PIM) in audio amplifiers, particularly that which may arise from the use of negative feedback, is considered. Coherent SMPTE-IM instrumentation capable of resolving two nanoseconds of equivalent time dispersion and measurement results from several different real amplifiers are presented. The results show that PIM is not a problem in contemporary amplifiers and that negative feedback reduces total PIM in most cases.

## 0. INTRODUCTION

Otala has reported the theory and some preliminary measurement results concerning phase intermodulation distortion (PIM) in audio amplifiers, particularly that which can result from the application of negative feedback. [1, 2, 3] In general terms, PIM can be described as phase modulation of a signal by accompanying signals. In comparison, the well-known phenomenon of amplitude intermodulation (AIM) distortion, often simply called IM, concerns amplitude modulation of a signal by accompanying

signals. Like AIM, PIM is a basically static distortion as opposed to dynamic distortions such as transient intermodulation distortion (TIM).

While investigations of PIM phenomena are new to the audio world, they are not new to the video community. There PIM and AIM are commonly referred to as differential gain and phase. Of particular importance to color transmission, differential gain and phase are routinely measured by impressing a small 3.58 MHz sinewave on an appropriate video test signal such as a ramp or staircase. A typical design objective for a transmission link would be one percent differential gain and one degree differential phase (peak-to-peak). Note that one degree at 3.58 MHz is approximately 0.78 nanoseconds.

The mechanism for feedback-generated PIM is quite straightforward when viewed with a simplified explanation as illustrated in Figure 1.<sup>3</sup> In essence, open-loop amplitude intermodulation (AIM) causes a signal-dependent variation of the amplifier's incremental open-loop gain. The high-frequency rolloff necessary for feedback compensation (usually 6 dB/octave) maps this into a signal-dependent closed-loop bandwidth which in turn results in signal-dependent closed-loop phase variation, or PIM. The assumption here is that the open-loop nonlinearities cause frequency-independent (i.e., flat) variation of open-loop

gain. While not all nonlinearities in all amplifier topologies behave this way, this explanation is still useful for our purposes here.

We should note that amplifiers normally produce a certain amount of PIM by mechanisms other than negative feedback, such as via nonlinear junction capacitances and signal-dependent power transistor bandwidth. These pre-existing PIM distortions will, as with other forms of distortion, generally tend to be reduced by the application of negative feedback. Therefore, in addition to assessing typical levels of PIM and estimating the seriousness of this impairment, a major objective here is to determine the net effect of negative feedback on total PIM. We will see that in many cases the reduction of pre-existing PIM by negative feedback exceeds substantially any PIM generated by negative feedback, resulting in a net improvement in the situation with the application of negative feedback.

Because negative feedback maps open-loop AIM into closed-loop PIM we expect there to be some theoretical linkage of levels of closed-loop AIM with closed-loop PIM, and this will be investigated. One might ask if negative feedback merely maps open-loop AIM into equally-bad closed-loop PIM, for example. We will show that the answer here is a clear no.

In order to facilitate meaningful experiments, a sensitive coherent SMPTE\* IM analyzer has been built which can measure both AIM and PIM. The addition of phase sensitivity to the standard SMPTE IM test has also been suggested by Otala. [3]

## 1. THEORY

Otala has shown that if an amplifier has an open-loop amplitude nonlinearity  $\epsilon(x)$  dependent on the signal  $x$  such that the open-loop gain is

$$A(x) = A_0 [1 + \epsilon(x)], \quad (1)$$

then the resulting feedback-generated phase dependency (PIM) in radians will be

---

\* Society of Motion Picture and Television Engineers.

$$\phi(x) = \arctan K \epsilon(x) \quad (2)$$

where

$$K = \frac{\omega}{\omega_{co}} \left[ 1 + \left[ \frac{\omega}{\omega_{co}} \right]^2 \right]^{-1}, \quad (3)$$

$\omega_{co}$  is the closed-loop cutoff frequency of the amplifier and  $\omega$  is the frequency of an infinitesimally small test signal whose phase modulation is of interest. [1]

This result was obtained by assuming that the open-loop nonlinearity is small [ $\epsilon(x) \ll 1$ ], memoryless, time-invariant and frequency-independent, that the feedback is large [ $(1 + BA_o) \gg 1$ ], and that the open-loop response of the amplifier has a single-pole rolloff. Although the situation in a real amplifier can be expected to be more complex, these assumptions are entirely reasonable for the purpose of gaining understanding of the phenomenon.

In order to gain some insight, we will now substitute some reasonable numbers. Suppose we have an amplifier with 10% open-loop nonlinearity and a closed-loop bandwidth of 1 MHz. What is the PIM at 20 kHz? Note that if this amplifier has a conventional 6 dB/octave open-loop rolloff it will have approximately 34 dB of feedback (F) at 20 kHz. We find that

$$K \approx \omega/\omega_{CO} \approx 1/F \quad (5)$$

and

$$\phi(x) \approx K \epsilon(x) \quad (6)$$

so that

$$\phi(x) \approx \epsilon(x) \omega/\omega_{CO} \approx \epsilon(x)/F \quad (\text{radians}) \quad (7)$$

and

$$t(x) \approx \epsilon(x)/\omega_{CO} \quad (\text{seconds}) \quad (8)$$

Turning to closed-loop AIM for comparison, if open-loop nonlinearities are reduced in proportion to the amount of feedback at frequency  $\omega$ , then this same amplifier could be expected to exhibit a closed-loop amplitude nonlinearity  $D(x)$  on the order of

$$D(x) \approx \epsilon(x)/F = .002 \quad (.2 \text{ percent}) \quad (9)$$

Comparing equations (7) and (9), it is quite apparent that there will be a strong linkage between closed-loop amplitude nonlinearity (AIM) and closed-loop phase nonlinearity (PIM) if feedback is the only source of PIM. If all of the above assumptions hold they are in fact numerically equal! Thus,

$$\phi(x) \approx D(x) \quad (10)$$

As a second example, suppose we have an amplifier whose SMPTE IM (60 & 6000 Hz, 4:1) measures .01%.\* Without even knowing the open-loop nonlinearity or the closed loop bandwidth (as long as they support the underlying assumptions) we can estimate the feedback-generated PIM to be (using Equations 10 and 4)

$$\phi(x) \approx .0001 \text{ radian}$$

$$t(x) \approx .0001/3.78 \times 10^4 = 2.3 \text{ nanoseconds} \quad (11)$$

With the above assumptions that closed loop AIM is reduced from open-loop nonlinearity by the amount of feedback at  $\omega$  and that the feedback factor is decreasing at 6 dB/octave over the region of interest, we expect closed-loop AIM to rise at 6 dB/octave with increases in  $\omega$  and

---

\* SMPTE IM is measured by applying 60 Hz and 6000 Hz signals in a 4:1 amplitude ratio to the unit under test (UUT) and measuring the amplitude modulation on the high-frequency signal at the output of the UUT.

feedback-generated PIM expressed in time to remain constant.

Although the real-world validity of the assumptions on which the above exercises are based (most of which are in the original theory presented by Otala) can be argued, the theory does provide a good basis for understanding the phenomenon of PIM due to negative feedback, including its relation to AIM, and shows that feedback-generated PIM in excess of about 20 nanoseconds should not be expected in amplifiers of reasonable design.

## 2. A COHERENT IM ANALYZER

A conventional SMPTE IM (AIM) analyzer normally consists of a signal source and product detector in one package. The signal source produces a low- and high-frequency tone pair (typically 60 and 6000 Hz or 60 and 7000 Hz) in an amplitude ratio of 4:1 at appropriate levels to drive the unit under test (UUT). The product detector portion contains a high-pass filter for removal of the low-frequency component, an average (envelope) detector for recovery of the modulation in the high-frequency component, suitable post-detection low-pass filtering and meter circuits. An automatic gain control (agc) circuit is often included prior to the detector to implement automatic level setting. In essence, it is little more than a specialized form of AM radio receiver. Because only simple, relatively



uncritical filtering is required, SMPTE IM analyzers can be made inexpensively and yet provide good sensitivity.

In principle, the detection of PIM in addition to AIM requires only that a phase detector be provided in addition to the existing amplitude detector. However, the phase detector must have a phase reference to work with, and so a fully coherent scheme involving synchronous detectors for both the amplitude and phase functions becomes attractive. The use of a synchronous detector for the amplitude function also tends to improve sensitivity to AIM through improved noise immunity as a side benefit.

The synchronous detectors are driven by a recovered 6 kHz "carrier" provided by a narrowband phase-locked loop. The amplitude and phase detectors differ only in the sense that they are driven by recovered carrier signals in quadrature with one another. These signals can be conveniently provided without extra hardware by the voltage-controlled oscillator (VCO) of the PLL.<sup>4</sup> The phase detector provided for recovery of the PIM information also conveniently serves as the phase detector for the PLL. The coherent IM analyzer detector portion is thus little more than a specialized form of coherent AM radio receiver.

Figure 2 shows a picture of the coherent IM analyzer actually constructed for this study and Figure 3 is

a simplified block diagram of the unit. It has an AIM measurement floor of 0.0015 percent and a PIM measurement floor of 1.2 nanoseconds. The output amplifier of the signal source is the only active stage in the system which must process the low and high frequency signals together. The use of a 5534 operational amplifier here assures extremely low residual intermodulation. Both measurement floors will increase somewhat depending on UUT noise contributions, but the coherent detection scheme does provide good immunity to this effect.

Most of the block diagram follows closely the description above. One important point in the practical realization which made the above performance achievable was the use of carefully designed, low-noise, highly stable state variable oscillators for the high-frequency source and the VCO or the PLL. In particular, low phase noise was of critical importance to the PIM detection process. Both state variable oscillators include highly linear agc circuits for leveling. Frequency control is achieved by varying the loop gain of the state variable oscillator by means of a low-distortion four-quadrant multiplier utilizing a JFET as the control element in a manner similar to that discussed for a state variable bandpass filter in Reference 4.

The low-pass filter following the low-frequency oscillator minimizes that oscillator's contribution of noise and harmonics to the test signal. Turning to the detector section, the 6th-order high-pass filter strongly attenuates the low-frequency component prior to the agc amplifier. Control voltage for the agc amplifier is conveniently supplied by the dc output of the synchronous AIM detector. By keeping the 6 kHz carrier at a constant level to the remainder of the analyzer, the agc permits level changes up to  $\pm 10$  dB at the input without affecting distortion calibration. The bandpass filter reduces the noise bandwidth of the carrier and further attenuates the low-frequency component prior to the detectors.

Sixth-order low-pass and second-order high-pass product filters eliminate the 12 kHz ripple from the detectors and suitably confine the measurement bandwidth to lie between one-half and five times the frequency of the low-frequency component. The high-pass product filter is especially important in reducing the effect of  $1/f$  phase noise produced by the oscillators.

In order to maximize flexibility, low frequency components other than the standard 60 Hz value are provided. These include 1 Hz, 5 Hz, 20 Hz and 200 Hz. It is felt that the lower test frequencies may prove especially useful in evaluation of distortion effects involving long time

constants, such as thermal feedback in operational amplifiers and thermal drift in power amplifier output stages. In addition to changing the frequency of the LF oscillator, this feature also requires that the cutoff frequencies of the product filters be made to track the selected frequency.

The one remaining block is the "PIM equalizer." In order that phase information be properly detected, the PLL must not track those phase changes. This implies the need for a narrowband PLL whose closed-loop bandwidth (often called its "jitter bandwidth") is well below the frequency of interest. While this is not difficult for 60 Hz modulation, an extremely narrow PLL would be required for the lowest modulation frequency of 1 Hz. Such a PLL would have a narrow capture range and a long capture time. Here we use a moderate-bandwidth PLL and employ the PIM equalizer to insert a 6 dB/octave boost below the frequency where PLL tracking inserts a 6 dB/octave rolloff.

For convenience, the complete analyzer also includes a sensitive (30  $\mu$ V full-scale) ac voltmeter function and optional noise-weighting filters ("A" and 20-kHz flat).

### 3. Measurements

In this section we will present several sets of measurements made using the coherent IM analyzer. These measurements are primarily intended to assess the level of PIM in real-world circuits and to answer some of the questions posed earlier. To put PIM in perspective, AIM (SMPTE-IM), 1 kHz total harmonic distortion (THD-1) and 20 kHz THD (THD-20) were measured as well. The measurements fall into three categories: First, several widely-used operational amplifiers were measured under representative operating conditions. Secondly, a 70-watt power amplifier of 1970 vintage and unsophisticated design was characterized to determine PIM levels in a fair (but not worst-case) example of power amplifier design. It is very unlikely that any contemporary amplifier of reasonable design would be much worse than this amplifier. Finally, an experimental power amplifier designed specifically for this project was evaluated. This amplifier can be operated with or without negative feedback and permits a just comparison of the PIM situation with and without negative feedback in basically the same circuit constructed at the same cost.

#### 3.1 Operational Amplifiers

Figure 4 shows the simple test circuit used to evaluate the operational amplifiers. It is an inverting

gain stage which can be operated at a gain of either minus one or minus ten. The use of an inverting topology eliminates the possible influence of common-mode distortion from the results.

Figures 5 through 11 show respectively the results for a 741 at unity gain, a gain of 10 and a gain of 10 with a heavier output load ( $R_L = 2.7K$ ); a 301 operated at a gain of 10 and appropriately compensated with 3 pf; a TL071 operated at gains of unity and 10; and a 356 operated at a gain of 10. The 741 is internally compensated for unity gain, while the 301 is a similar device employing external compensation. The TL071 and 356 are FET-input operational amplifiers internally compensated for unity gain. The highly-acclaimed 5534 bipolar operational amplifier was also measured at a gain of 10, but the distortion was so low that no plots were necessary: PIM and AIM were below the measurement floor (0.0015 percent and 1.3 nanoseconds in this situation) almost to the clipping point even into a 600 ohm load with  $\pm 12$  volt supplies.

Turning to the plots, first note that all of the operational amplifiers were operated from  $\pm 12$  volt power supplies and that PIM is plotted in nanoseconds on the right-hand scale. The results are summarized in Table 1 at a single rms operating level of 6 volts. None of the operational amplifier data shows any surprises. Notice,

however, that it is difficult to correlate the Table 1 results with Equation 10, partly because so much of the AIM and PIM data is at the residual level. It also suggests that the operational amplifier distortion mechanisms may not fit the assumptions of Section 1.

All of the devices tend to exhibit very low values of the static distortions (THD-1, AIM and PIM), while 20 kHz THD has the usual strong dependency on device slew rate. As expected, the distortion levels tend to rise with operating level and are greater in the times-ten situation for the unity-gain compensated devices.

Even the much-criticized 741 at a gain of 10 with normal loading exhibits less than four nanoseconds of PIM, and under heavy loading still shows less than nine nanoseconds of PIM. It is worth noting that in the times-ten situation the closed-loop bandwidth of the 741 is only about 100 kHz. The 301 and TI071 at a gain of 10 performed very well on all measures. Although the 356 exhibits substantial second-harmonic THD-20, it performs very well on the static tests. One additional point notable from the operational amplifier data is that PIM distortion seems relatively insensitive to clipping, while AIM is quite sensitive to it.

With the worst PIM less than 10 nanoseconds, the

above data suggest that PIM is not a problem in operational amplifiers.

### 3.2 Existing Power Amplifier

Data for the 1970-vintage power amplifier is shown in Figure 12. As mentioned earlier, this is not a high-performance amplifier. It employs a simple, fairly conventional circuit with 1 MHz  $f_t$  output transistors in a quasi-complementary output stage, achieves a slew rate of about 4 V/ $\mu$ s, and produces substantial transient intermodulation distortion. The closed-loop bandwidth of the amplifier is about 300 kHz. The THD-20 data in Figure 12 give further evidence of the poor dynamic performance of this amplifier. The THD-1 and AIM curves, respectively showing 0.1 and 0.36 percent distortion levels just below clipping, indicate that this amplifier is a dubious performer in terms of static distortion as well.

With this background information we should conclude that this amplifier will exhibit considerable PIM. It does, compared to the operational amplifiers. However, it is quite notable that PIM is still only 25 nanoseconds at the onset of clipping where AIM is 1.7 percent. At lower levels PIM is less than 10 nanoseconds. We again see that PIM is rather insensitive to soft clipping. Given this benign level of PIM distortion on such a poor example of



amplifier design, we must wonder if PIM is of any consequence in any power amplifiers of reasonable design.

### 3.3 Experimental Power Amplifier

Figure 13 is a schematic of the experimental 35-watt power amplifier built specifically for this project. Without the dotted elements the amplifier performs without any negative feedback other than that provided by local emitter degeneration. With the dotted components included and the pair of 8.2 kilohm predriver collector load resistors removed, the amplifier functions as a conventional design incorporating substantial negative feedback. In the latter configuration, the amplifier exhibits a closed-loop bandwidth of 600 kHz, 30 dB of feedback at 20 kHz and 60 to 70 dB of feedback at low frequencies. The design incorporates a complementary predriver and a complementary triple-Darlington output stage, but is not unusually sophisticated compared to existing contemporary designs. The type of feedback compensation employed makes the amplifier essentially a non-slew-limited design. Slewing is not evident on a 40 Vp-p 100 kHz unfiltered squarewave into an 8 ohm load, and is probably in excess of 80 V/ $\mu$ s.

Figure 14 shows distortion performance for the no-feedback version. The static THD-1 and AIM distortions are not unreasonable for an unsophisticated no-feedback

design and show no surprises. Most of the distortion is from the output stage, which is slightly overbiased. Notice that AIM is about three times as sensitive to this as THD-1. Over most of the range, THD-20 is only moderately greater than THD-1. PIM is, as expected, non-zero even though there is no overall negative feedback. It climbs smoothly with level to about 50 nanoseconds prior to clipping.

Figure 15 shows the same data for the version with feedback. As expected, THD-1 and AIM are dramatically reduced by a factor of 30, while THD-20 is reduced by a smaller factor of eight. PIM was reduced with the application of negative feedback by a factor of six to a level of only 8 nanoseconds just prior to clipping. Reduction of PIM by feedback at medium levels was closer to a factor of three. This data shows clearly that, while negative feedback may in principle generate some PIM, the reduction of pre-existing PIM by feedback will usually result in an overall reduction of PIM rather than an increase of PIM in contemporary power amplifiers of reasonable design.

The oscilloscope photos in Figures 16 and 17 illustrate the AIM and PIM distortion waveforms respectively for the version with feedback operating at an rms level of 15V. Due to an extra inversion in the analyzer's AIM product channel, the sense of the waveform is such that a

positive modulation (gain increase) causes a negative deflection. The crossover distortion results from a slight overbiasing which causes a slight gain increase in the crossover region. The slight delay of the product's negative peak from the crossover point is due to the low-pass filtering in the analyzer.

In an earlier paper<sup>3</sup> it was suggested that PIM is a sensitive indicator of crossover distortion, so measurements were taken on the above feedback amplifier in a seriously underbiased condition which produced classic Class B crossover distortion effects. The data is shown in Figure 18. While distortion at high levels is not markedly different from the previous case, there is a considerable increase in all forms of distortion at low levels as expected. Figures 19a through d show the THD-1, THD-20, AIM and PIM distortion products respectively at an rms operating level of 0.5V, corresponding to 31 milliwatts into 8 ohms. The distortions increased from the previously-biased condition by the following factors at this level: THD-1: 6; THD-20: 50; AIM: 12; PIM: 31. Note that some of the distortions in the previous condition were at the equipment residual. This data and the photographs suggest that THD-20 and PIM are somewhat better indicators of crossover distortion. Even under this condition, however, PIM was only 37 nanoseconds.

#### 4. Conclusion

The mechanism of phase intermodulation distortion (PIM) created by negative feedback has been investigated and its strong linkage to other static distortions has been illustrated. It was also pointed out that PIM arising from mechanisms other than negative feedback may dominate in many situations. This latter PIM will be subject to reduction by negative feedback, often resulting in a net reduction in PIM with the application of negative feedback.

A sensitive means of measuring PIM incorporating a coherent SMPTE IM analyzer has been developed. Capable of measuring PIM with a noise floor or less than 1.2 nanoseconds, the instrument also results in improved measurement of conventional SMPTE-IM (AIM) with a noise floor of about 0.0015 percent.

Experimental results carried out on several operational and power amplifiers indicate that while PIM is a useful and sensitive performance indicator, PIM distortion does not appear to be a problem in real amplifiers unless the ear has the capability of detecting time dispersion on the order of 10 nanoseconds. It also appears that the occurrence of PIM will always be accompanied by substantial amounts of more conventional intermodulation and harmonic distortions. This likelihood should not escape careful

consideration in any listening experiments which are performed to assess subjective effects of PIM.

#### REFERENCES

1. M. Otala, "Feedback-Generated Phase Modulation in Audio Amplifiers," 65th Convention of the Audio Engineering Society, London, 1980, Preprint No. 1576.
2. M. Otala, "Conversion of Amplitude Nonlinearities to Phase Nonlinearities in Feedback Audio Amplifiers," Proc. of IEEE International Conference on Acoustics, Speech and Signal Processing, Denver, CO, 1980, pp. 498-499.
3. M. Otala, "Phase Modulation and Intermodulation in Feedback Audio Amplifiers," 68th Convention of the Audio Engineering Society, Hamburg, 1981, Preprint No. 1751.
4. R. R. Cordell, "Build a High-Performance THD Analyzer," Audio, Vol. 65, Nos. 6-9, July -September, 1981.

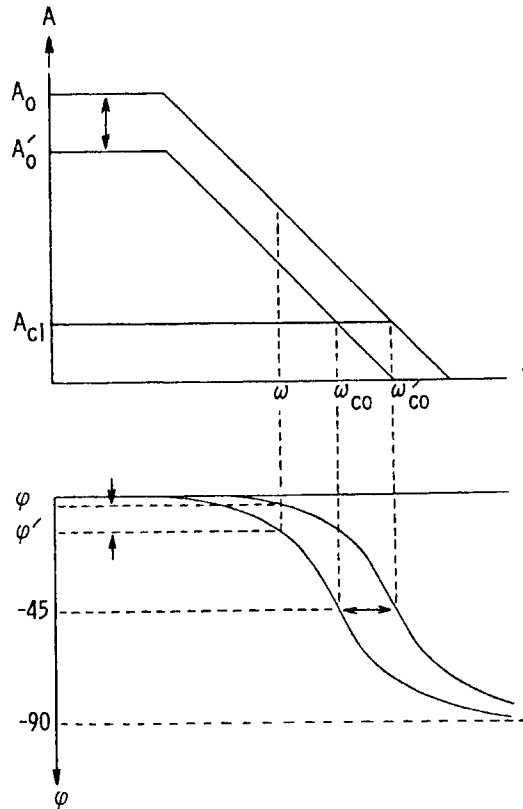


FIGURE 1: Diagram illustrating the conversion of open-loop amplitude nonlinearities to closed-loop phase nonlinearities via negative feedback.<sup>3</sup>

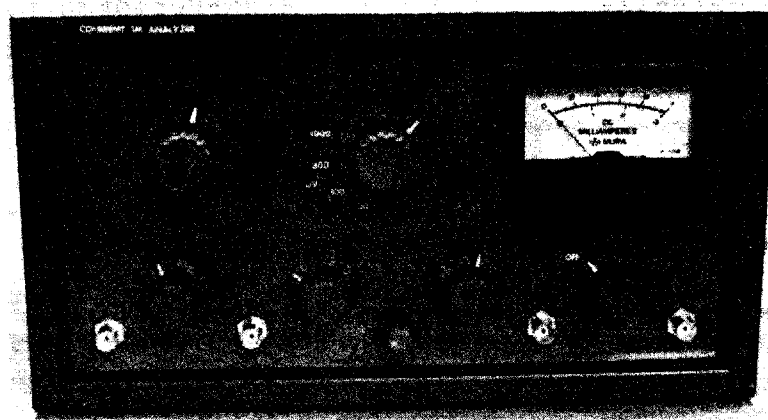


FIGURE 2: Photograph of the coherent IM analyzer developed to measure both SMPTE IM (AIM) and phase intermodulation (PIM) distortion.

# COHERENT IM ANALYZER

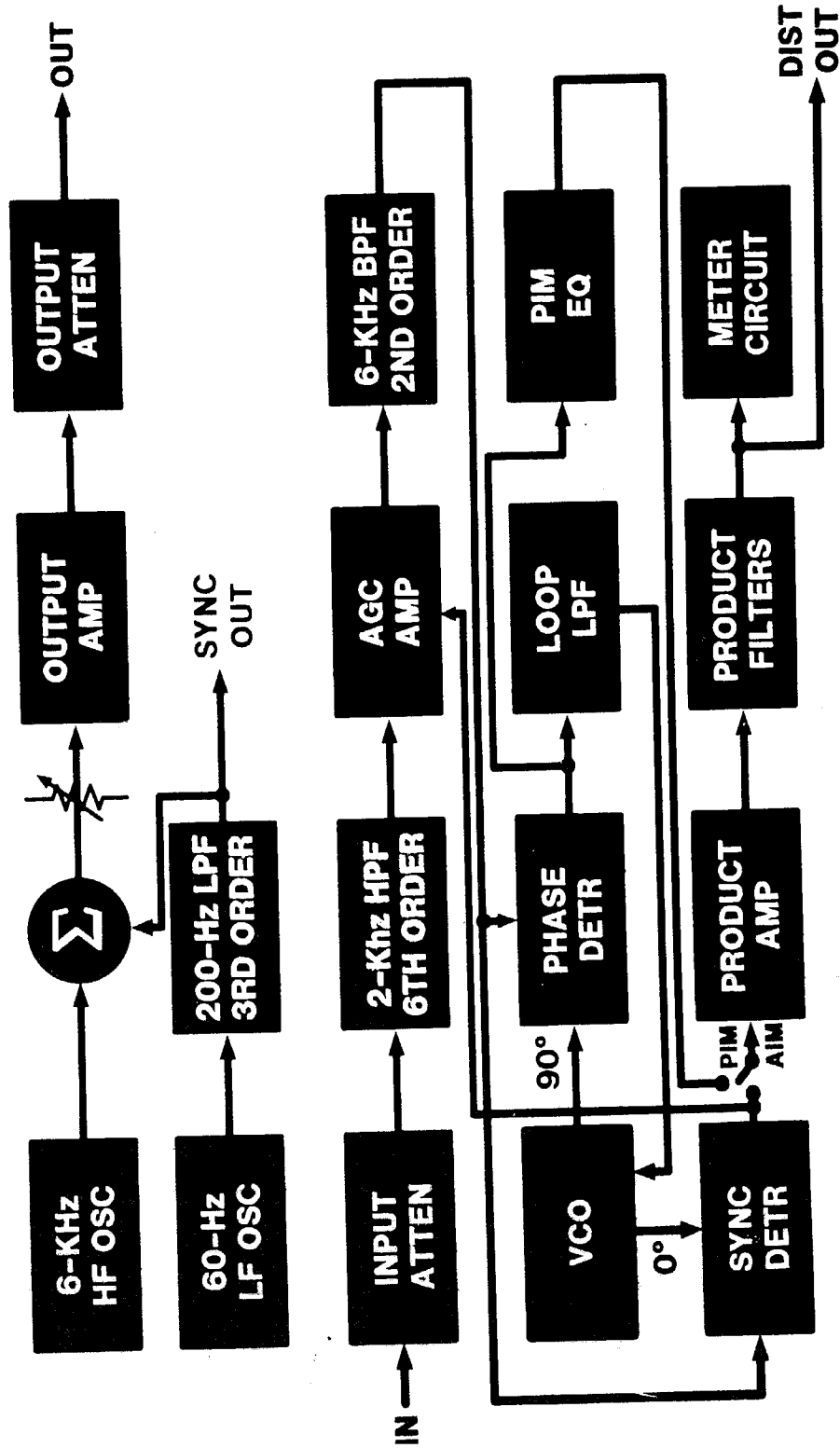


FIGURE 3: Simplified block diagram of the coherent IM analyzer. The use of synchronous detection including a phase detector permits detection of phase intermodulation distortion in the SMPTE IM format.

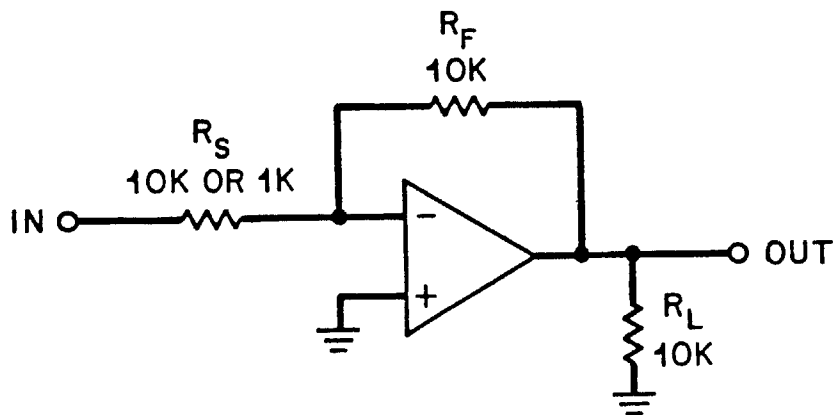


FIGURE 4: Test circuit used to evaluate distortion of operational amplifiers. All units were operated from  $\pm 12$ -volt power supplies at an inverting gain of one or ten.

<u>DEVICE</u>	<u>GAIN</u>	<u>THD-1(%)</u>	<u>THD-20(%)</u>	<u>AIM(%)</u>	<u>PIM(<math>\mu</math>s)</u>
741	-1	.0008	> 8	.0017	<.0012
741	-10	.0028	> 8	<.0016	.0039
741*	-10	.0065	> 8	.0032	.0088
301	-10	<.0008	.012	<.0015	<.0012
TL071	-1	.0006	.003	.002	<.0011
TL071	-10	.001	.013	<.0017	.0016
356	-10	<.0008	.048	<.0016	<.0011

\* $R_L = 2.7K$

< INDICATES INSTRUMENT RESIDUAL.

TABLE 1: Summary of operational amplifier performance at an rms operating level of 6 volts ( $\pm 12V$  supplies).



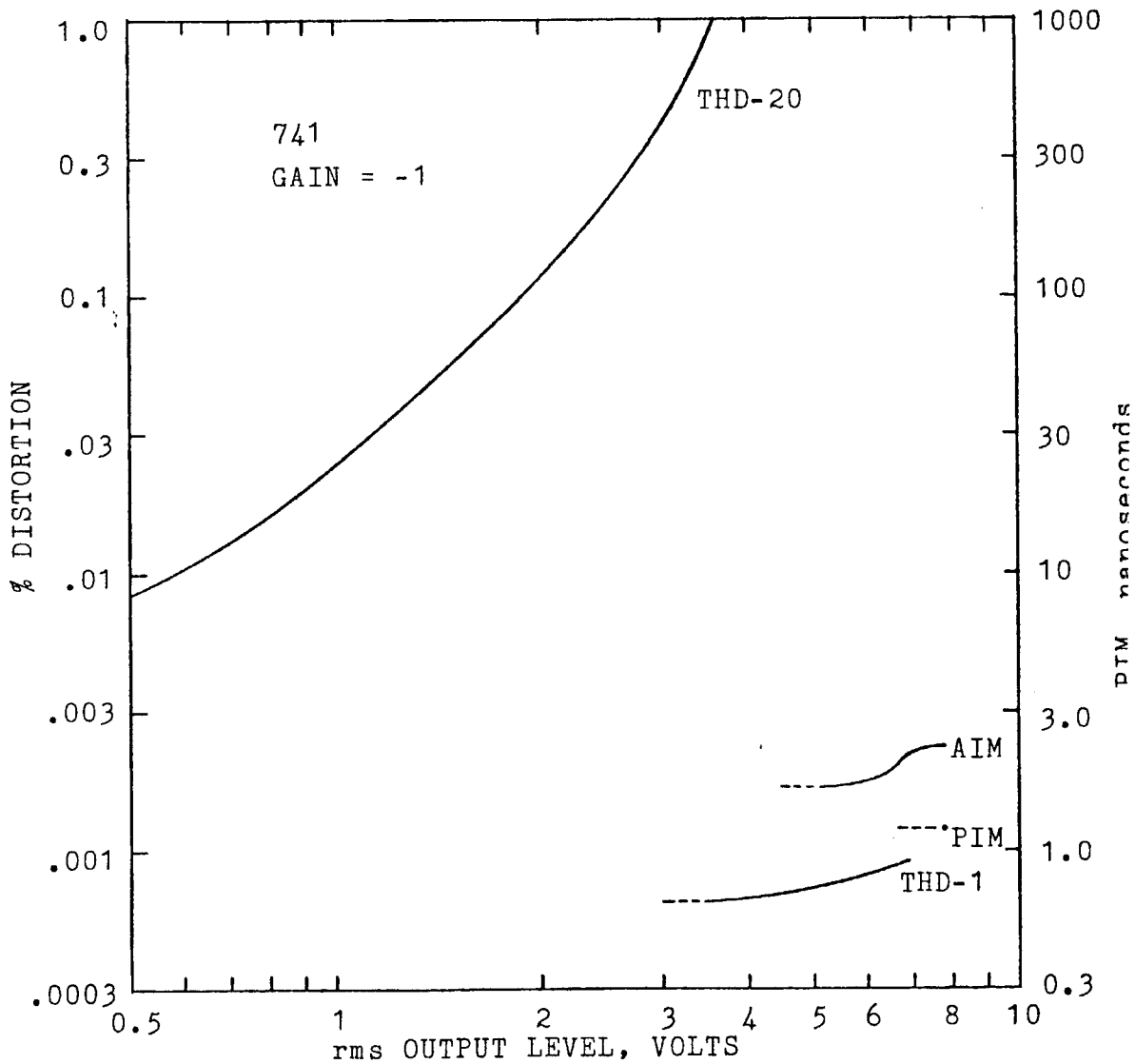


FIGURE 5: Performance of a 741 operational amplifier at unity gain. Note that PIM is expressed in nanoseconds on the right-hand scale. Dashed line indicates point at which measurement residual is reached.

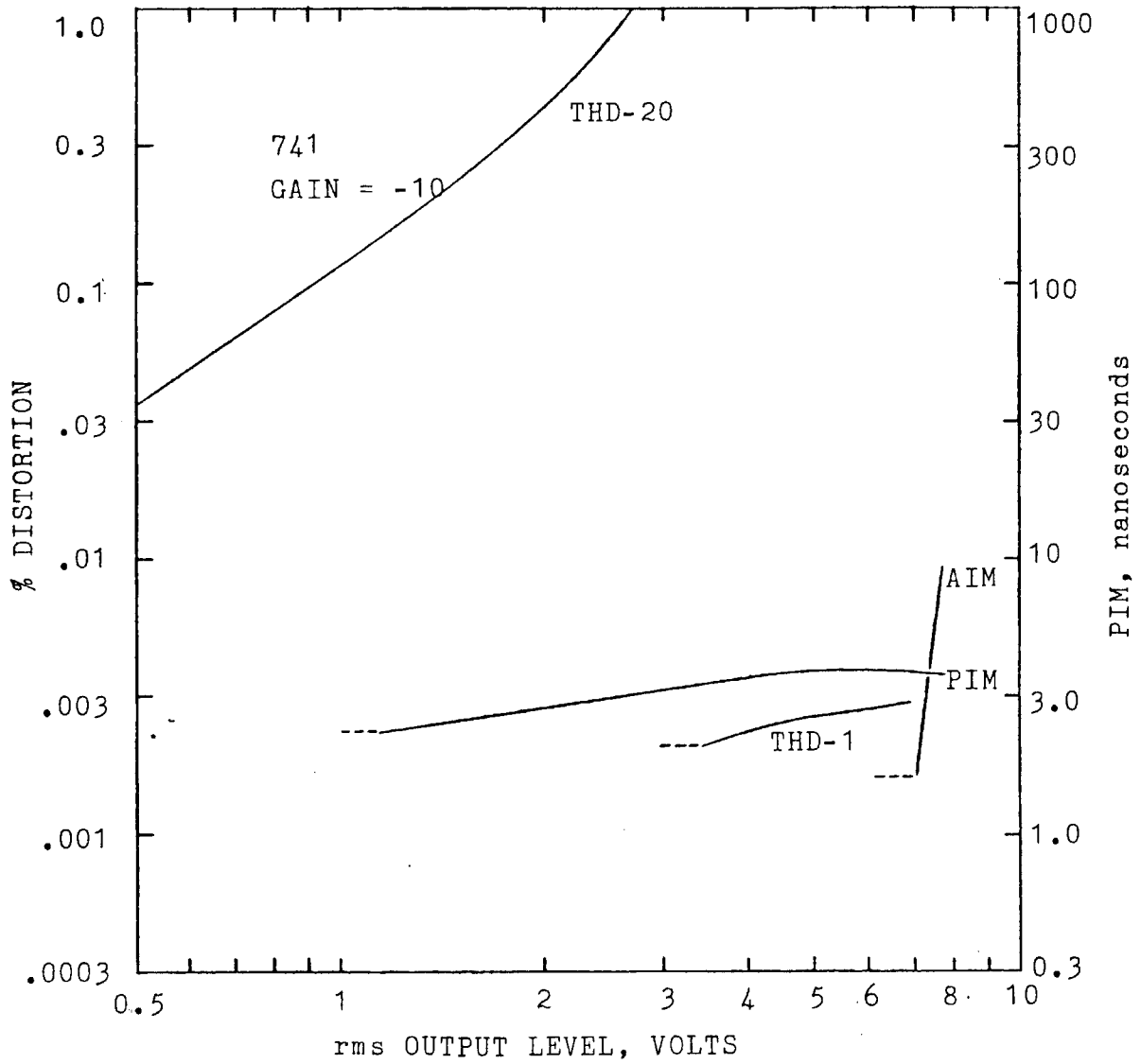


FIGURE 6: Performance of the 741 operational amplifier at a gain of ten. Note increased distortion levels due to decreased negative feedback.

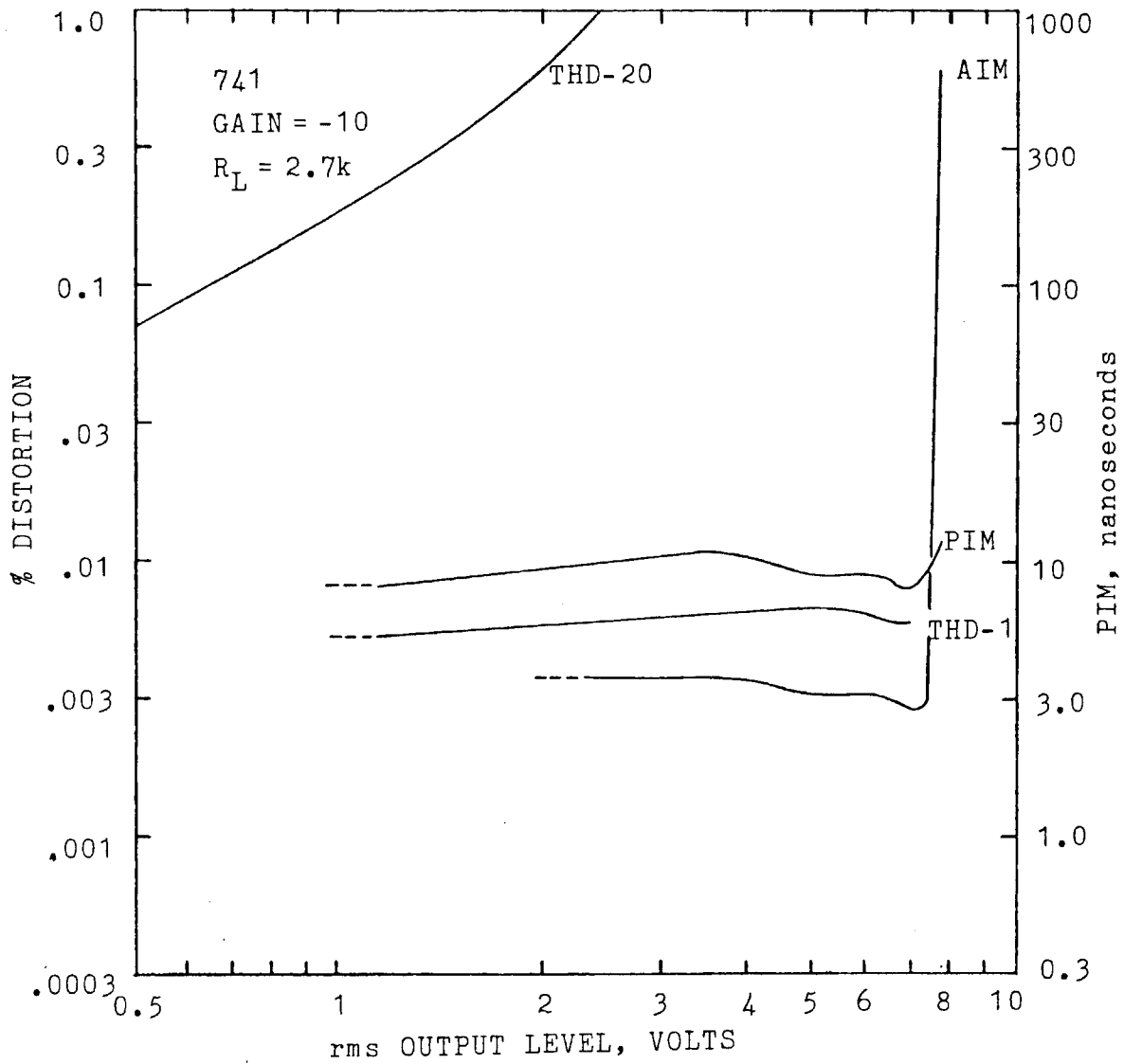


FIGURE 7: Performance of the 741 operational amplifier at a gain of ten as in Figure 6, but with a heavier output load ( $R_L = 2.7k$ ) resulting in higher distortion.

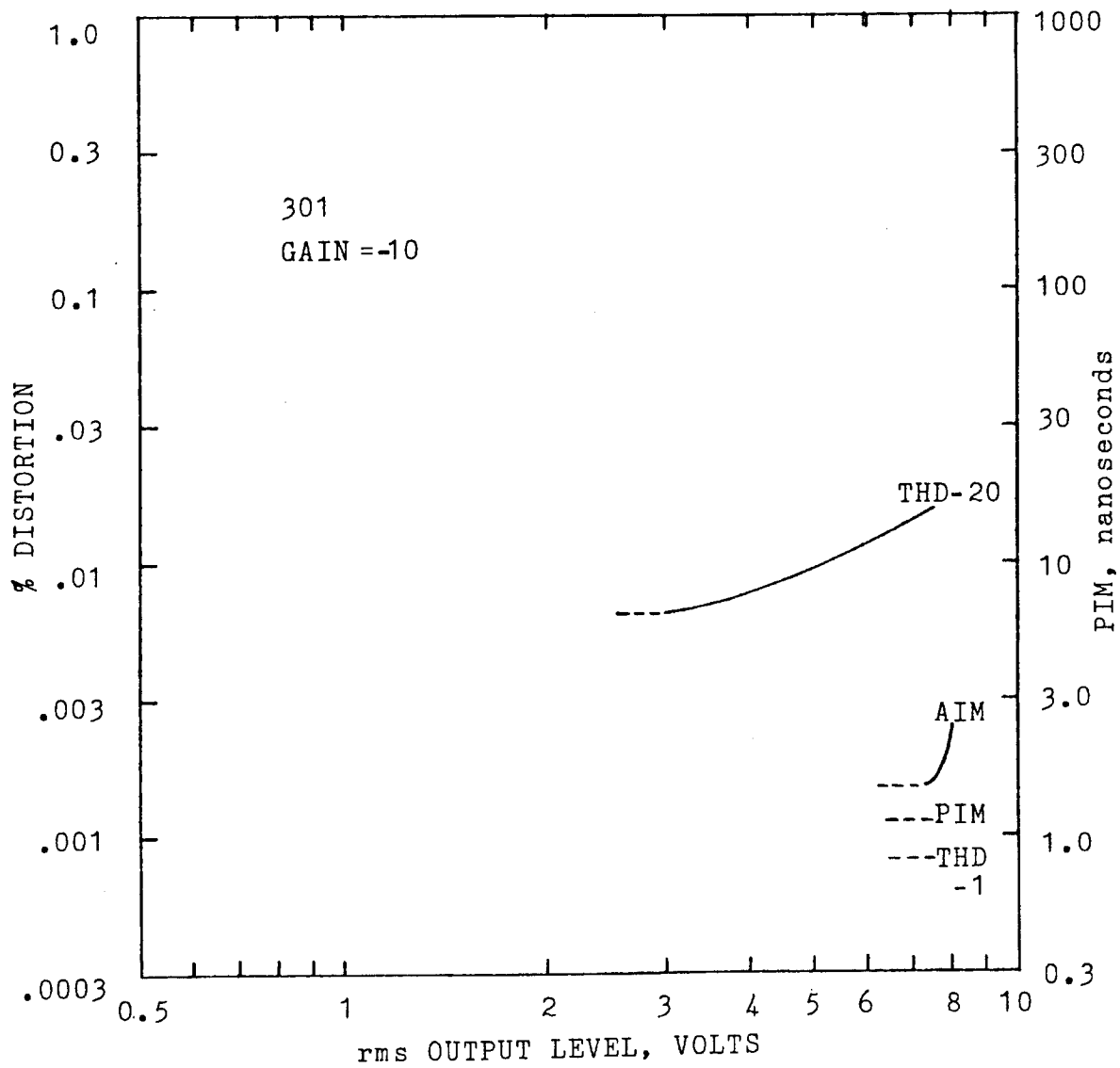


FIGURE 8: Performance of a 301 operational amplifier at a gain of ten and optimally compensated with 3 pf. Improved performance results from increased negative feedback with the lighter compensation.

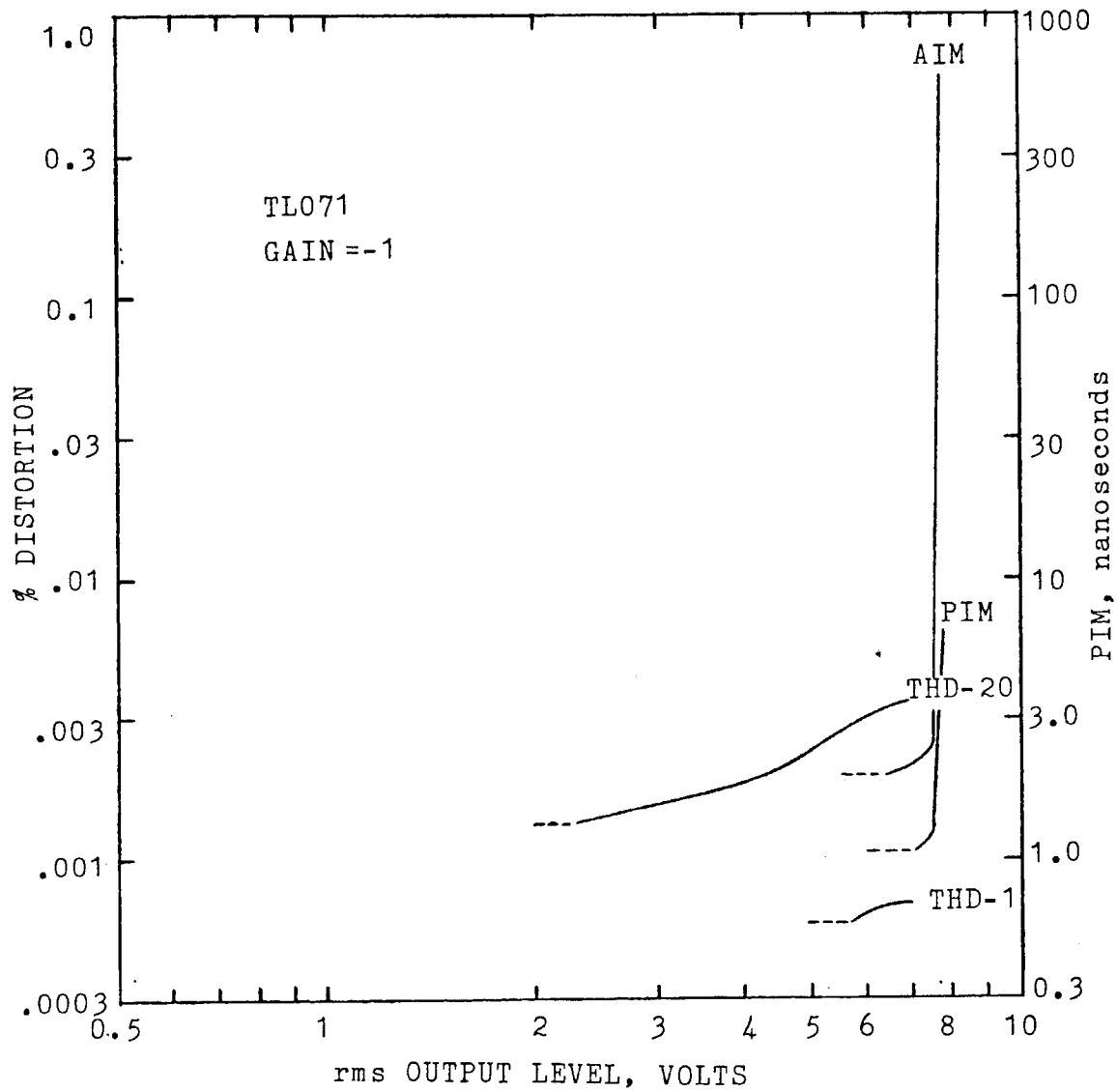


FIGURE 9: Performance of a TL071 FET-input operational amplifier at unity gain.

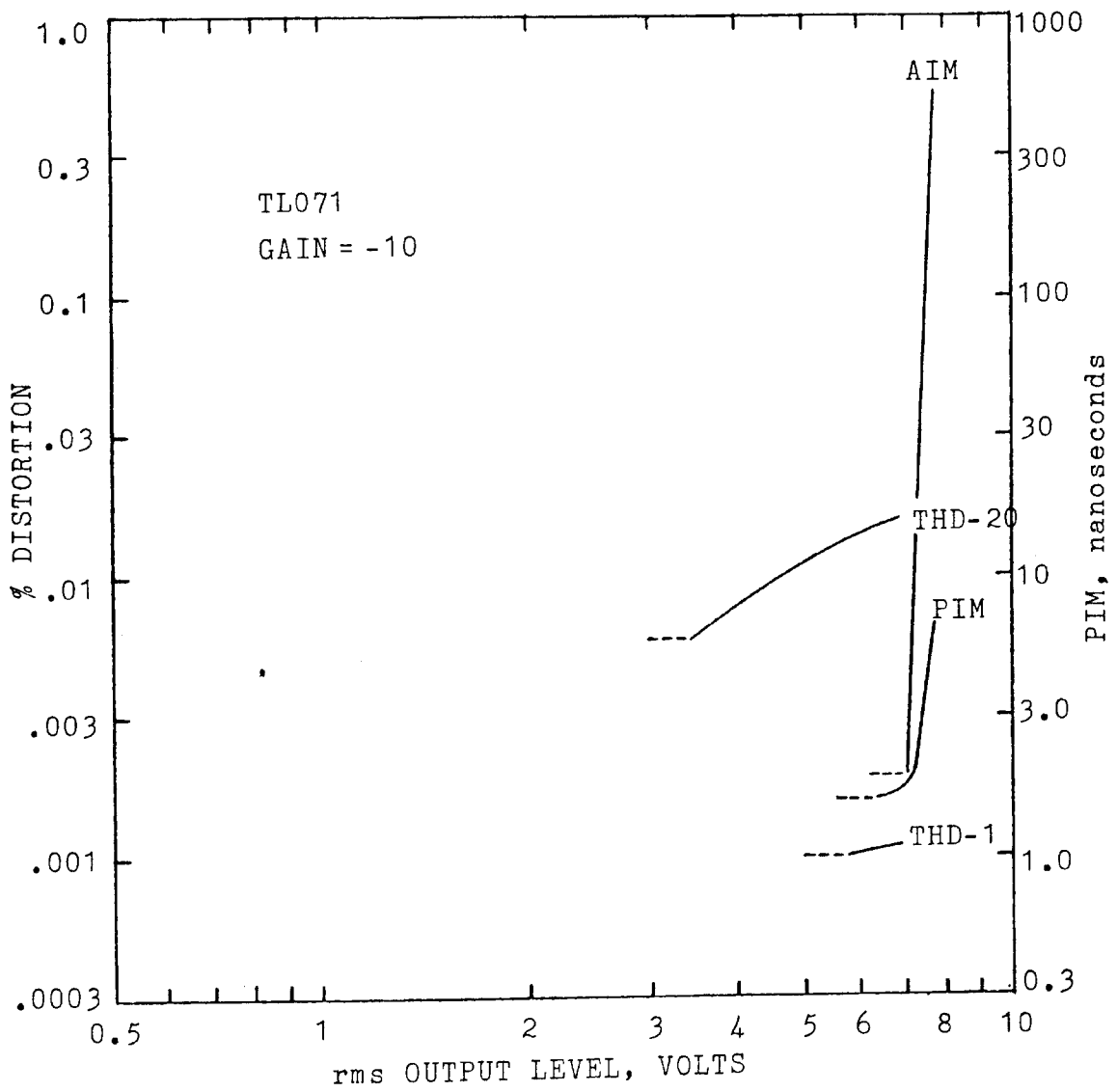


FIGURE 10: Performance of the TL071 FET-input operational amplifier at a gain of ten. Performance is excellent in spite of the fixed unity-gain internal compensation.

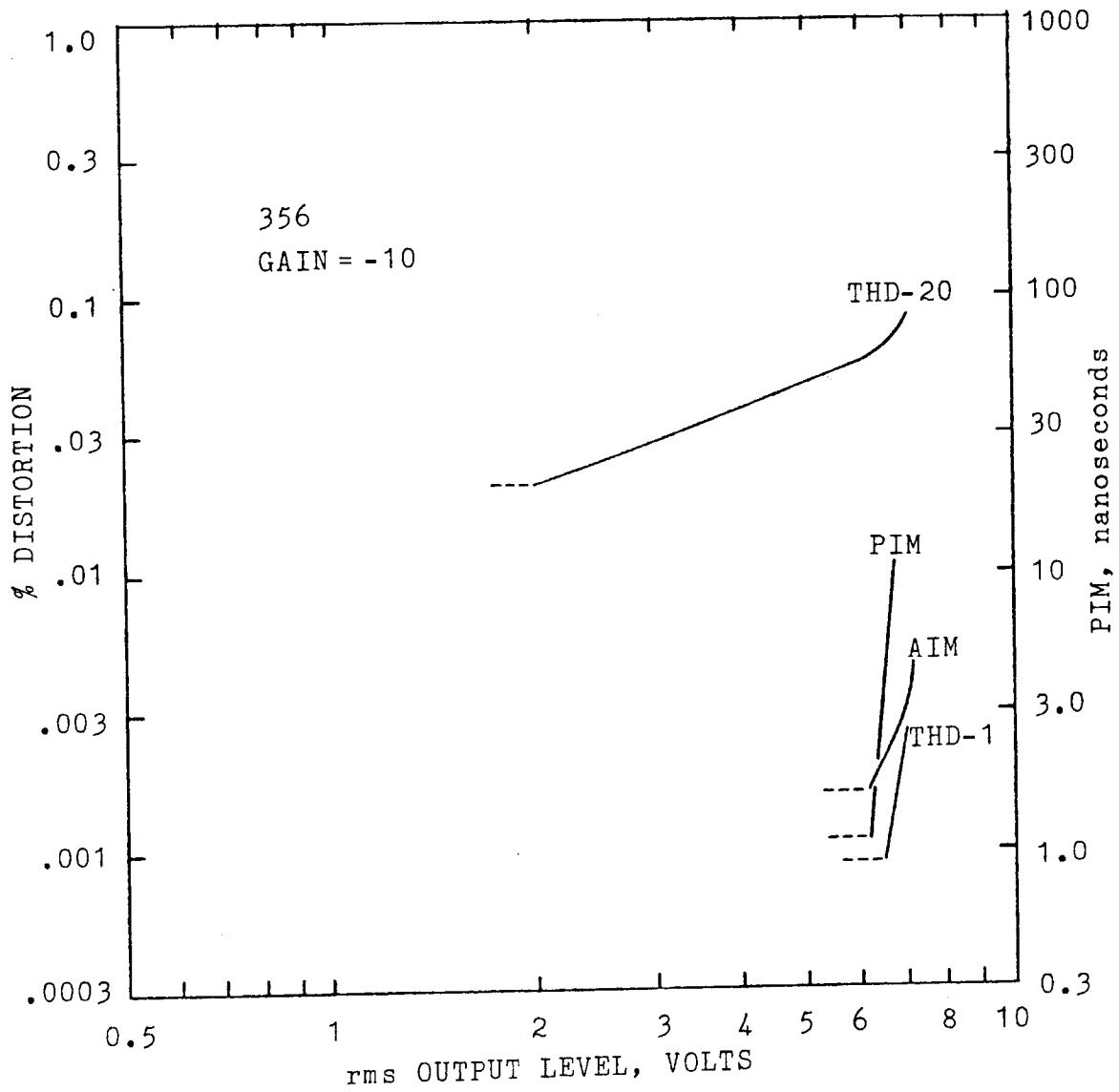


FIGURE 11: Performance of the 356 FET-input operational amplifier. The moderate THD-20 is primarily second harmonic.

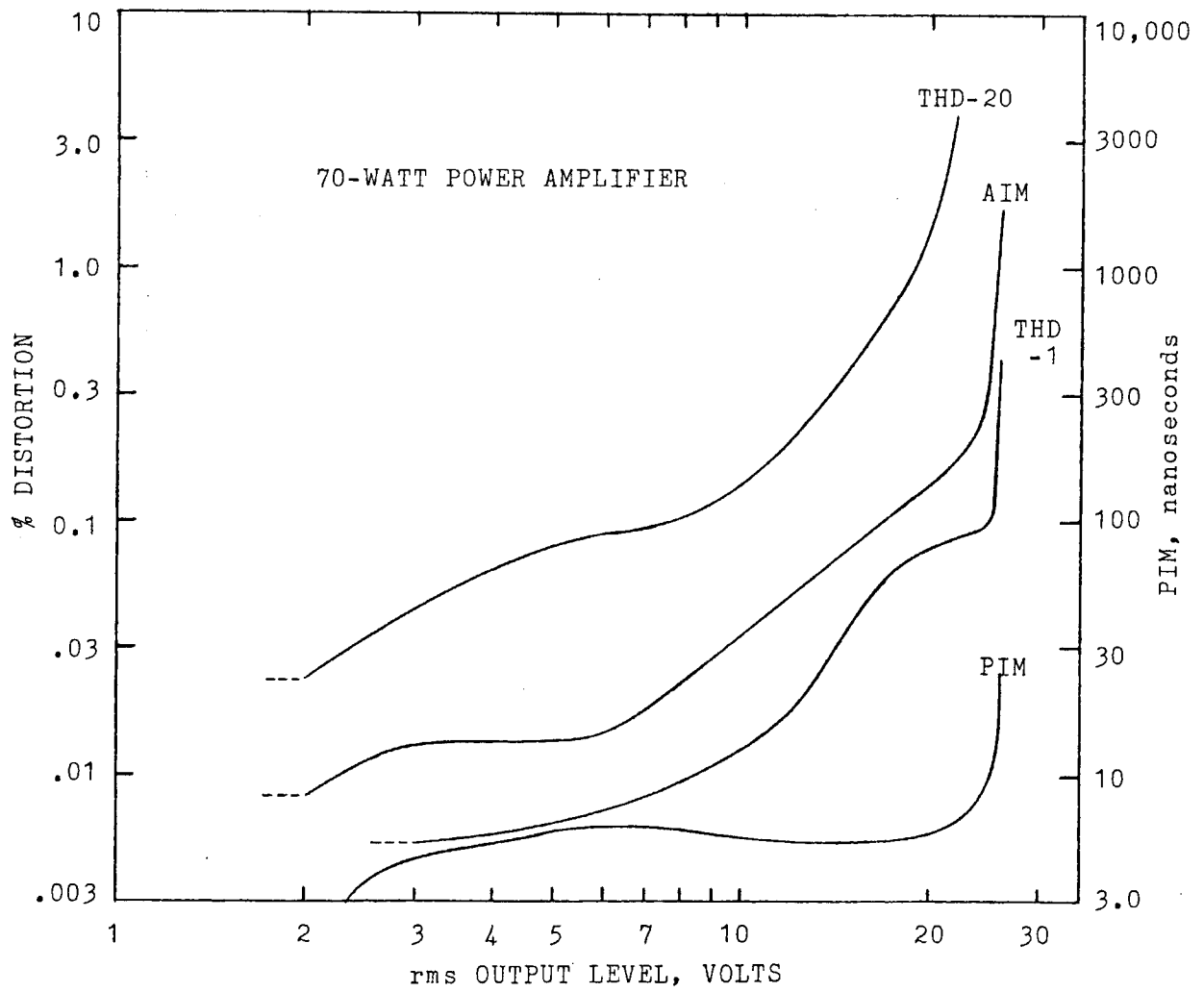


FIGURE 12: Performance of a 70-watt power amplifier of 1970 vintage and unsophisticated design. Even here PIM is less than 10 nanoseconds below clipping.



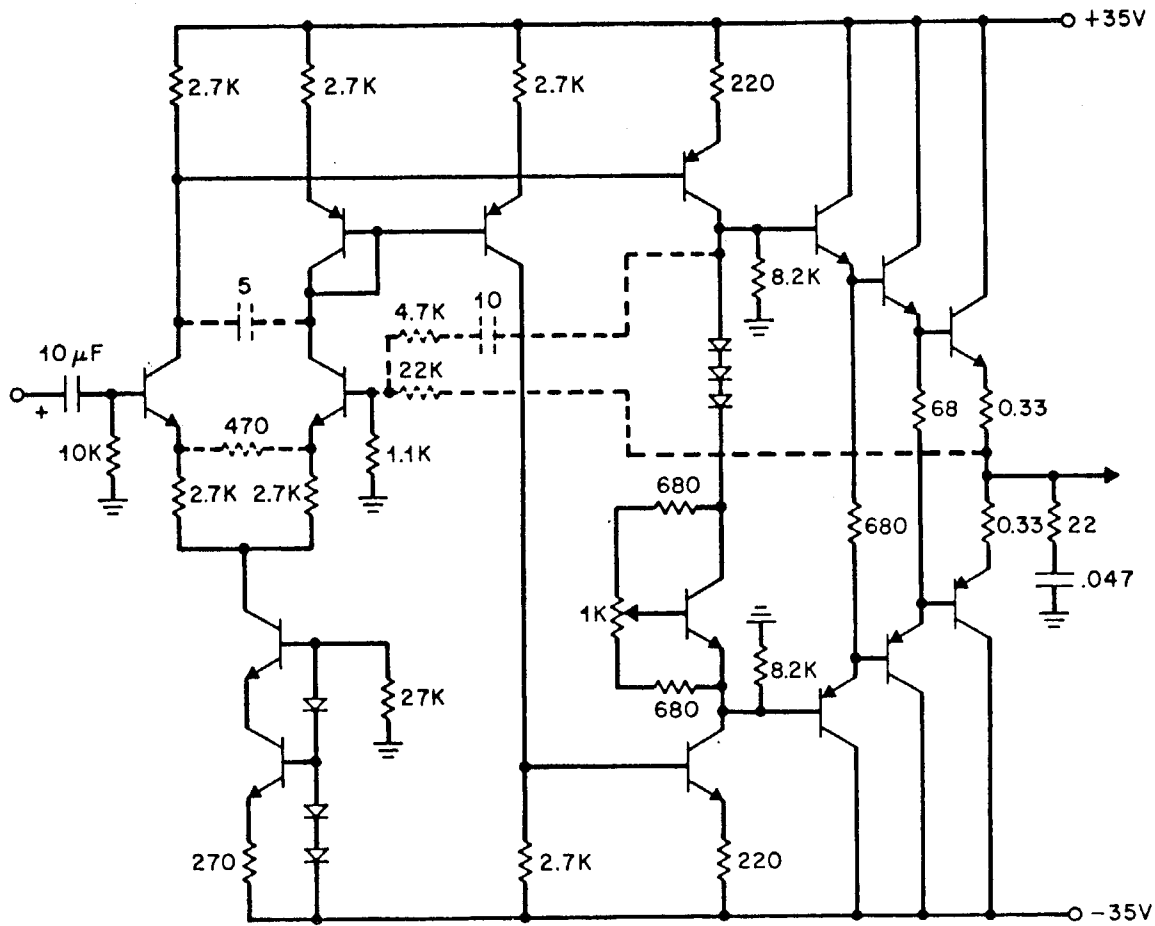


FIGURE 13: Circuit of the experimental 35-watt power amplifier which operates with or without overall negative feedback depending on use of dashed elements and predriver load resistors.

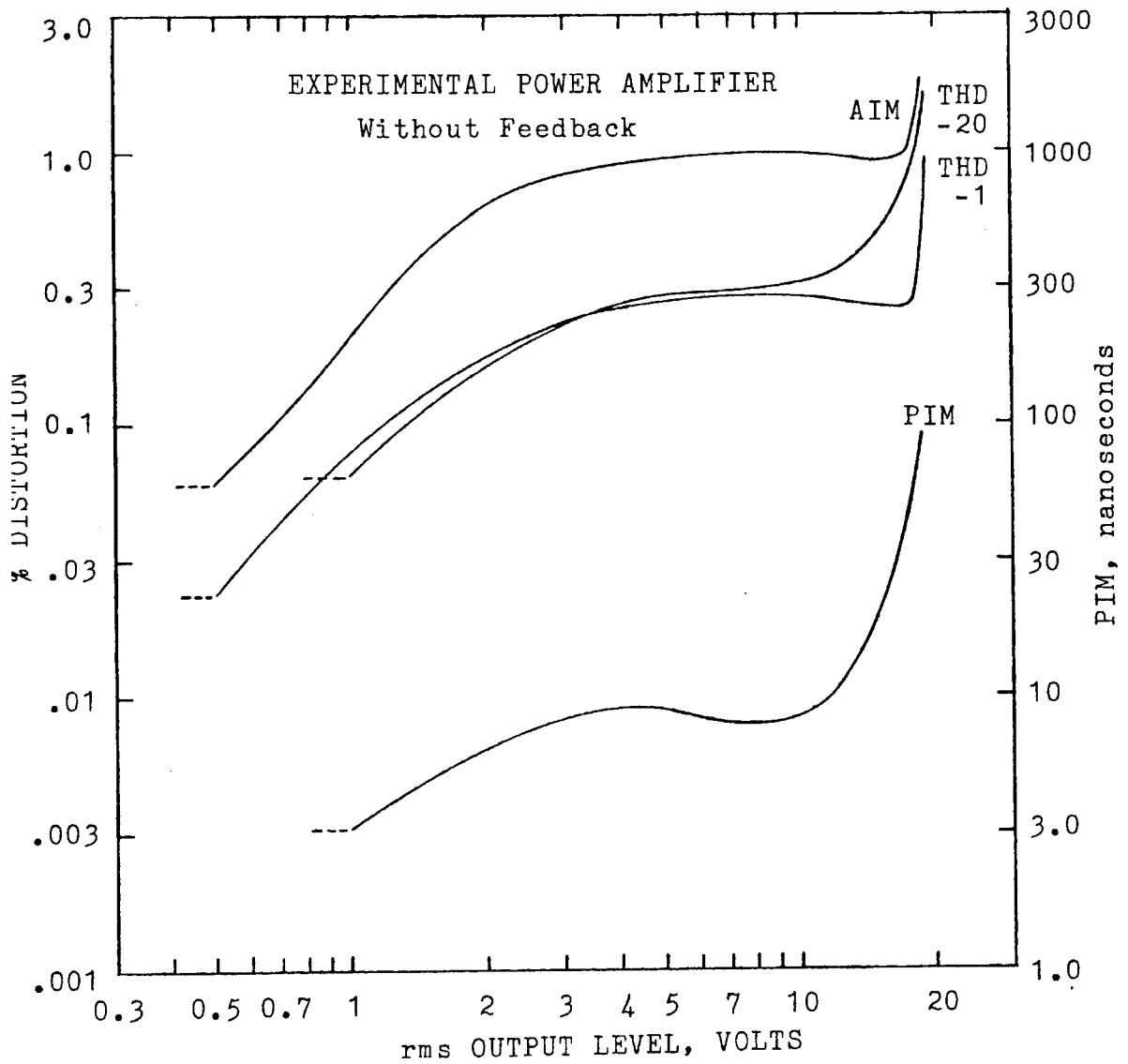


FIGURE 14: Performance of the experimental power amplifier without feedback. Crossover distortion due to slight overbiasing of the output stage is the major contributor. Non-feedback-generated PIM rises to 50 nanoseconds just prior to clipping.

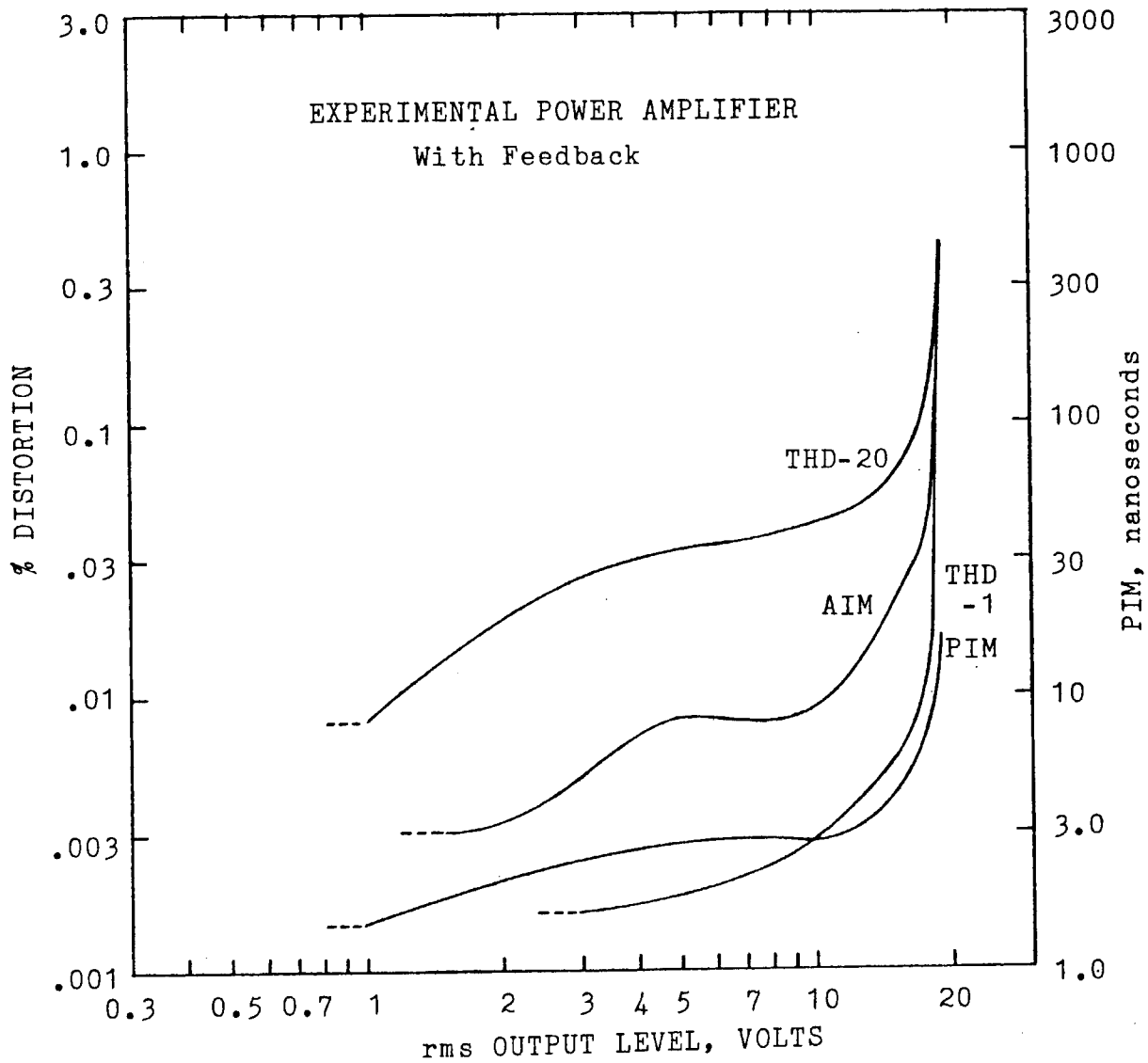


FIGURE 15: Performance of the experimental power amplifier with negative feedback. Compared to Figure 14, total PIM is reduced by a factor of three to six with feedback.

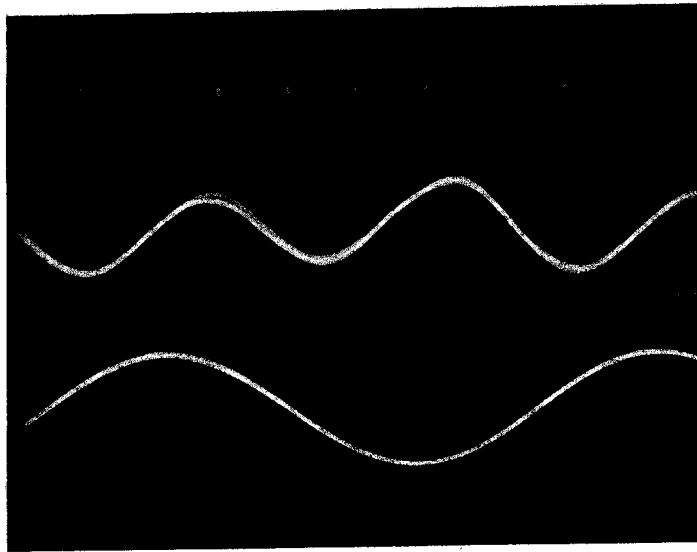


FIGURE 16: AIM distortion waveform for the experimental power amplifier operating with negative feedback at an rms level of 15 volts into eight ohms (top trace). Bottom trace is 60 Hz sync.

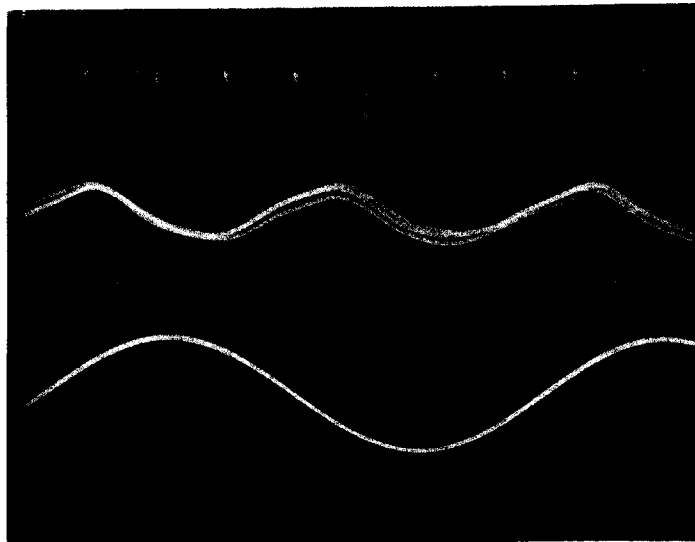


FIGURE 17: PIM distortion waveform for the experimental power amplifier operating with negative feedback at an rms level of 15 volts into eight ohms (top trace).

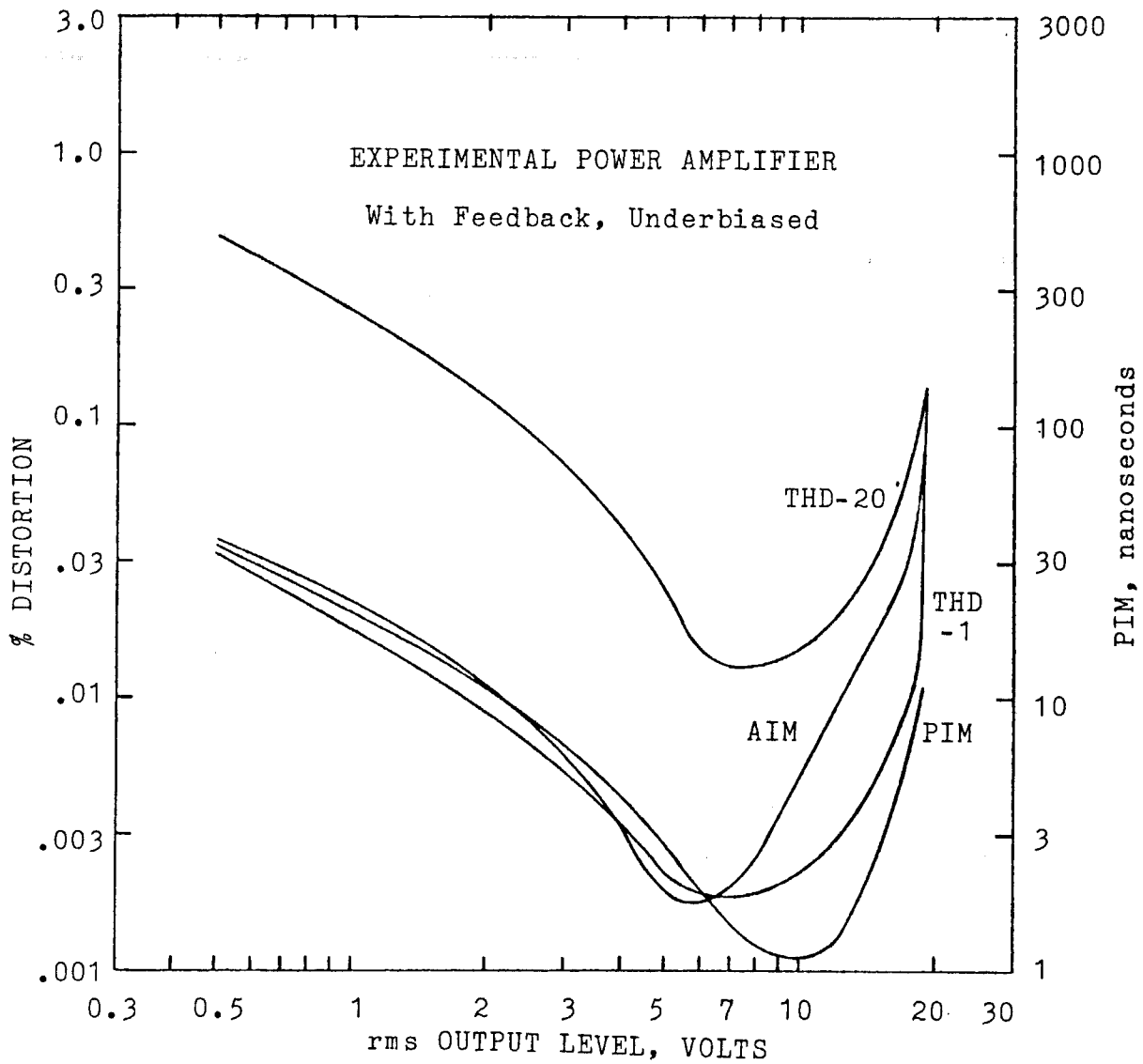
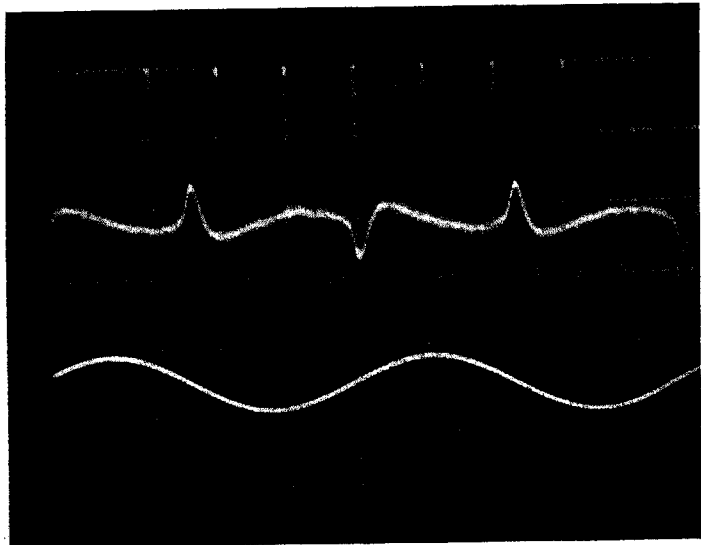
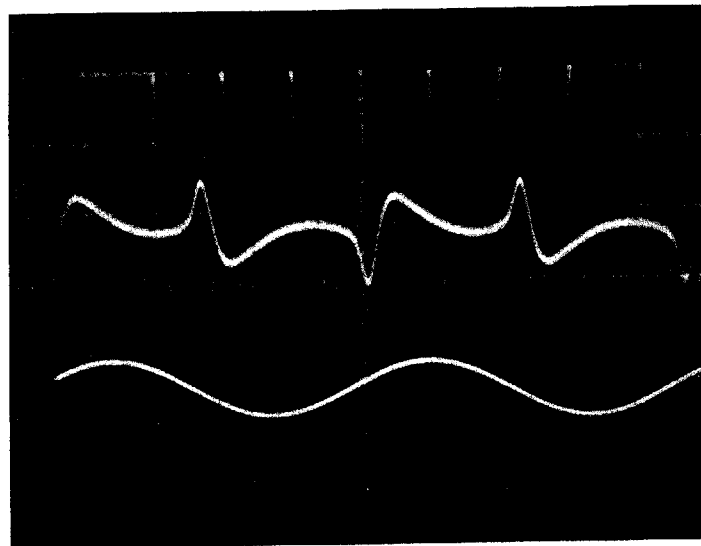


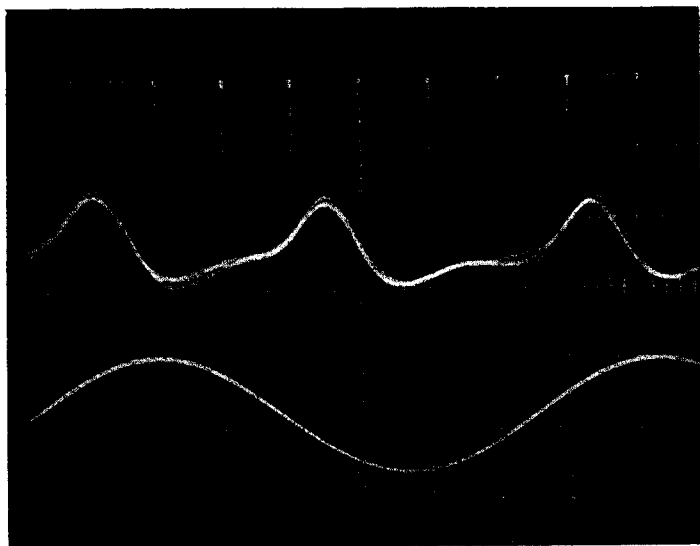
FIGURE 18: Performance of the experimental power amplifier in an underbiased condition producing crossover distortion. Rising distortion at low levels indicates crossover distortion.



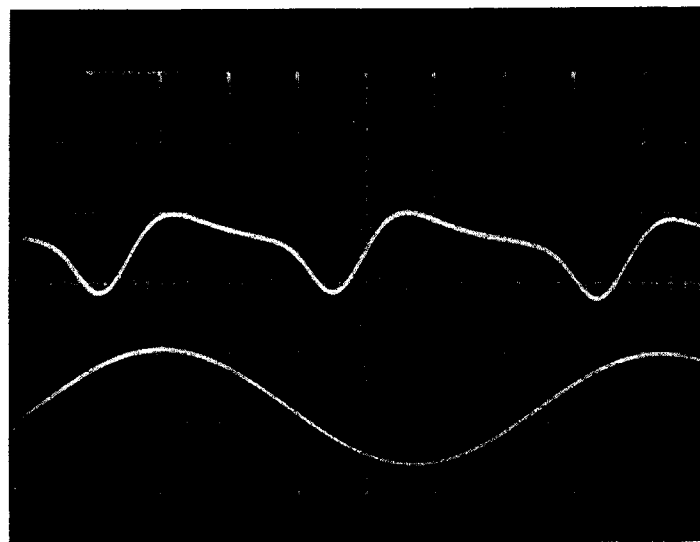
(a)



(b)



(c)



(d)

FIGURE 19: Distortion waveforms for the underbiased amplifier operating at an rms level of 0.5 volt into eight ohms (top trace). (a) THD-1; (b) THD-20; (c) AIM; (d) PIM. THD-20 and PIM are somewhat more sensitive to the crossover distortion.